*Biomacromolecules* **2006,** *7,* 2890−2900

# Macromolecular Assemblies Based on Coupled Inclusion Complex and Electrostatic Interactions

Virginie Burckbuchler, Valérie Boutant, Véronique Wintgens, and Catherine Amiel*

*Laboratoire de Recherche sur les Polymères, LRP, C.N.R.S. UMR 7581, 2-8 rue Henri Dunant, 94320 Thiais, France*

*Received May 30, 2006; Revised Manuscript Received July 27, 2006*

Macromolecular assemblies are elaborated by mixing $\beta$-cyclodextrin-containing polymer (poly$\beta$CD), dextran sulfate polyanion (NaDxS), and cationic amphiphiles which are adamantane derivatives (Ada1 or Ada2) in aqueous medium. These components are assembled via coupled inclusion complex interactions (adamantyl group with cyclodextrin cavity) and electrostatic attractive interactions (positive charges of Ada with negative charge of NaDxS). The structural properties are studied by viscometry and small angle neutron scattering. Ternary aggregates with larger size and lower compacities are observed as the cation concentration is increased, until phase separation occurs. The results are in good agreement with a core−shell association mechanism, the core being made of one poly$\beta$CD chain, the shell of NaDxS chains, and the Ada amphiphiles being distributed more or less homogeneously inside the cyclodextrin cavities. The nature of the Ada counterions has a strong influence on the association as Ada1 with $I^-$ counterions give smaller and less compact aggregates than Ada2 with $Br^-$ counterions.

## Introduction

Supramolecular architectures involving polymers constitute an area of current interest and development due to their practical applications in the design of stimuli-responsive gels[1] or nanoparticles[2] that could be used for drug delivery or gene therapy and, in the case of interfacial modifications, in the design of biosensing devices.[3,4] The driving interaction mechanisms leading to polymer−polymer associations can be classified in 3 types: (a) hydrophobic interactions occurring in aqueous systems of amphiphilic copolymers,[1,2,5] (b) electrostatic interactions between polymers of opposite charges,[6] responsible of well-defined polyelectrolyte multilayers at interfaces,[7] (c) interactions involving a molecular recognition process such as hydrogen bond interactions in proteins[8,9] or inclusion complexes with $\beta$-cyclodextrin compounds.[10−16]

Cyclodextrins (CD) are cyclic oligomers of anhydroglucose with the shape of a truncated cone that has a hydrophilic exterior and a less polar cavity in the center. $\alpha$, $\beta$, and $\gamma$-cyclodextrins consist respectively of 6, 7, or 8 glucose units. In aqueous solutions, cyclodextrins form inclusion complexes with substances containing lipophilic groups, provided that the shape of the hydrophobic group fits in the cavity.[17,18] For instance, the adamantyl group precisely fits into the $\beta$-cyclodextrin cavity.[19]

$\beta$-Cyclodextrin ($\beta$CD) units, due to their specific interaction with well chosen hydrophobic guests, can be used as tools to build tailorable macromolecular assemblies. $\beta$-CD are integrated over polymeric architectures (poly$\beta$CD) in order to ensure multiple interactions with the guests. Lock and key systems have been built by mixing in aqueous solution poly$\beta$CD and hydrosoluble polymers containing hydrophobic guests.[15,20−22] These polymer couples interact via inclusion complexes, and the strength of the interaction is largely controlled by the density of links between the two polymers. Depending on the number of hydrophobic groups per chain of guest polymers, soluble complexes, nanoparticles, or phase-separated systems can be obtained.[20,22] The $\beta$CD units in these systems do not only play a role in building the nanoassemblies but can also trap hydrophobic drug molecules for drug delivery applications.

Cyclodextrin polymers have also found interest in the field of gene therapy.[23−26] The first requirements for the gene vectors are their ability to condense DNA and to overcome the electrostatic repulsions to the negatively charged membrane cells. Davis and co-workers have synthesized positively charged polymers containing $\beta$-cyclodextrin units in their backbone.[23] These polymers condense DNA via electrostatic interactions, like other cationic polyelectrolytes, the principal role of the $\beta$CD units being to lower the toxicity of the gene carrier. The $\beta$CD units also served as potential sites for surface modification of the colloidal structures via inclusion complexation. Poly(ethylene glycol) modified at one end with an adamantyl moiety (Ad-PEG) was found to stabilize the particles through the formation of PEG brushes, whereas PEG modified at both ends with an adamantyl moiety and a targeting ligand (Ad-PEG-L) was used for cell targeting.

More complex systems using a combination of electrostatic and inclusion complex interactions have been designed. For instance Yui and co-workers have synthesized $\beta$-cyclodextrin conjugated poly($\epsilon$-lysine).[27] These cationic polymers are able to interact with anionic amphiphiles via both host−guest and electrostatic complexation thus leading to pH and temperature responsive supramolecular structures. In this study, the macromolecular assemblies are elaborated from a ternary system: a neutral $\beta$CD polymer, a cationic amphiphile, and an anionic polymer are mixed together in aqueous media. The cationic amphiphiles act as connectors between the two polymers as they make inclusion complexes with the $\beta$CD cavities of the poly$\beta$CD and interact electrostatically with the anionic polymer. Potential applications of these systems are in gene delivery, DNA being the anionic polymer. Compared to the gene carriers prepared using cationic copolymers,[28] our systems provide

---

* To whom correspondence should be addressed. Tel: +33(0)1 49 78 12 19. Fax: +33(0)1 49 78 12 08. E-mail address: amiel@glvt-cnrs.fr.

10.1021/bm060523k CCC: $33.50

several advantages including the easy charge ratio control by the adjustment of the connector's concentration and an improved dissociation of the complexes realized either by screening the Coulombic interactions or by dissociating the inclusion complexes. These systems could also provide interesting carriers for negatively charged proteins.

Previous works have demonstrated the occurrence of the ternary complexes using dextran sulfate, polystyrene sulfonate and DNA fragments as different models of polyanions, a branched $\beta$-cyclodextrin epichlorohydrin polymer (poly$\beta$CD) and dodecyltrimethylammonium chloride (DTAC) as the cationic amphiphile. The studies have shown that the connector's concentration ($N_{\mathrm{DTAC}}$) played a major role in the structural properties of the complex. A structural transition from diffuse aggregates at low $N_{\mathrm{DTAC}}$ to compact aggregates at higher concentration occurred at a critical DTAC concentration ($N_{\mathrm{DTAC}}^{\mathrm{crit}}$). This structural transition of the ternary complexes has been related to a change of the DTAC distribution along the poly$\beta$CD chains in the binary complexes poly$\beta$CD/DTAC: from an inhomogeneous distribution at low surfactant concentration, the DTAC being distributed along a spherical outer shell of the poly$\beta$CD, to a more homogeneous distribution beyond $N_{\mathrm{DTAC}}^{\mathrm{crit}}$. Some of the questions that remain unanswered from the previous studies are related to the nature of the connector. DTAC is a cationic surfactant able to self-associate and form hydrophobic microdomains. Although previous studies have shown that hydrophobic self-assembling of the surfactants is not the main association mechanism in the ternary systems, their contribution as competitive or cooperative effects cannot be ruled out. The aim of this paper is to study the influence of the connector's nature. Connectors with no self-association properties have been synthesized using adamantane-based amphiphiles. The bulkiness of the adamantyl groups prevents them from making large hydrophobic microdomains as do alkyl tails. Another aim of this work is to study the influence of a spacer between the charge and the hydrophobic group on the decoupling of the electrostatic and inclusion complex interactions. Two connectors (Ada1 and Ada2) differing in the length of the spacer have been synthesized. To be able to compare our results to the ones obtained with DTAC, the experiments have been performed using dextran sulfate (NaDxS) ($M_w = 40\,000$) as the polyanion and the same poly$\beta$CD as in the previous works.

The paper will start with a first study of the binary interactions poly$\beta$CD/Ada (Ada stands for Ada1 or Ada2) and Ada/NaDxS. It will be shown that careful analysis of the binary systems constitutes a necessary step to understand the interaction mechanisms in the ternary systems (second part). The structural properties of the binary and ternary systems are studied by viscometry and neutron scattering.

## Experimental Section

**Materials.** The polyanion sodium salt dextran sulfate (NaDxS) was supplied by Sigma (St Quentin Fallavier, France). Its sulfur content is 17% which corresponds to about two sulfate groups per glucose unit and its weight-average molecular weight is 40 000 g mol$^{-1}$.

The poly-$\beta$-cyclodextrin polymer (poly$\beta$CD) was synthesized by polycondensation of $\beta$−cyclodextrin with epichlorohydrin under strong alkaline conditions.[29] The sample was purified by ultrafiltration of aqueous solutions on membranes of molecular weight cut off 30 000. It was characterized by size exclusion chromatography coupled with light scattering detector: its weight-average molecular weight and its polydispersity index are $M_w = 160\,000$ g mol$^{-1}$ and $M_w/M_n = 1.9$, respectively. Its $\beta$CD content, determined by $^1$H NMR, is 59 wt %.

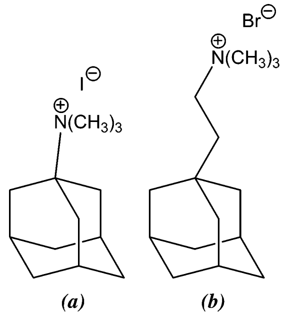

**Figure 1.** Chemical structures of the cations (a) Ada1 and (b) Ada2.

The two cationic connectors were synthesized in the laboratory and their structures are shown in Figure 1. 1-Adamantyl trimethylammonium iodide (Ada1) was prepared following a one-step procedure using a described method.[30] A total of 2.5 g of 1-adamantylamine (Aldrich) was dissolved in 20 mL of dimethylformamide, and 8 mL of tributylamine (Aldrich) were added. Then 4.2 mL of iodomethane was slowly added. The mixture was left under stirring at room temperature for 24 h. The white solid sample was filtered, washed with acetone and diethyl ether, and finally dried. The obtained 1-adamantyl trimethylammonium iodide (26% yield) was characterized by $^1$H NMR ($D_2O$): 1.6 (m, 6H); 2.0 (m, 6H); 2.25 (m, 3H); 2.9 (s, 9H). The synthesis of 1-(1-adamantyl)-2-trimethylammoniumethane bromide (Ada2) has already been reported.[26]

**Fluorescence Measurements.** A SLM Aminco 8100 fluorimeter was used for the fluorescence experiments. A fluorescent probe, 4-amino-*N*-*tert*-butylphthalimide, able to make inclusion complexes with CDs, was used as a competitor for Ada1 and Ada2.[31]

For the association constants determination, a stock solution of the probe in water (around $5 \times 10^{-5}$ M) was prepared and used to make a $10^{-2}$ M poly$\beta$CD solution in order to have the same probe concentration; then mixtures of these two solutions were used to record the fluorescence at different poly$\beta$CD concentrations (with excitation wavelength located at the isosbestic point (414 nm) to avoid any optical density variation). This allowed the determination of $K_{\mathrm{probe}} = 5900$ M$^{-1}$. For the competition experiments, a stock solution of the probe with appropriate poly$\beta$CD concentration ($1/K_{\mathrm{probe}} \sim 2 \times 10^{-4}$ M) was prepared and used to make a concentrate solution of the competitor ($5 \times 10^{-3}$ M); again mixtures of these two solutions were used to record the fluorescence at different competitor concentrations. This allowed the determination of $K_{\mathrm{Ada}}$ (complexation constant between competitor and poly$\beta$CD).

**Viscometric Measurements.** The viscosity of the solution was determined with an Ubbelohlde viscometer at 25 ± 0.05 °C in a thermostated bath. Samples were previously filtered over a Minisart RC15 Sartorius with 0.45 $\mu$m porosity. All of the dilutions were directly performed into the viscometer.

**SANS Measurements.** The SANS experiments were carried out with the PACE spectrometer at the Laboratoire Léon Brillouin (LLB), Saclay, France. The experimental scattering vector $q$ ($q = (4\pi/\lambda)\sin(\theta/2)$) range was $0.0032 < q$ (Å$^{-1}$) $< 0.12$ and was covered by two sample-to-detector distances (3 m at the neutron wavelength of 6 Å$^{-1}$ and 5 m at 13 Å$^{-1}$). The wavelength dispersion $\Delta\lambda/\lambda$ of the velocity selector was 10%. The samples were kept in quartz cells (Hellma) with a path length of 2 mm for samples in $D_2O$. The collected data were normalized for the detector efficiency using the isotropic scattering of a 1 mm thick calibration sample of $H_2O$. The raw data were corrected for background from the solvent and sample cell. All of the samples were prepared in $D_2O$ to maximize the contrast between the $\beta$-cyclodextrin polymer ($\rho_{\mathrm{poly}\beta\mathrm{CD}} = 2.29 \times 10^{10}$ cm$^{-2}$) and the solvent ($\rho_{D2O} = 6.41 \times 10^{10}$ cm$^{-2}$). The scattering length densities of Ada1, Ada2, and the dextran sulfate are $0.30 \times 10^{10}$, $0.22 \times 10^{10}$, and $1.75 \times 10^{10}$ cm$^{-2}$, respectively (without the counterions).

## Results

**1. Binary Complexes.** Ada1 and Ada2 are expected to form inclusion complexes with $\beta$-cyclodextrin through the hydrophobic adamantyl group. Adamantane derivatives are known to form stable complexes with $\beta$-cyclodextrin as the size of this group perfectly fits the $\beta$CD cavity. High association constants of the order of $10^4-10^5$ M$^{-1}$ have been reported.[32] On the other hand, Ada1 and Ada2 may strongly interact with NaDxS through electrostatic interactions. Therefore, Ada1 and Ada2 will form binary complexes either with poly$\beta$CD or with NaDxS.

*1.1. Determination of the Association Constant of the poly$\beta$CD/Ada1 or Ada2 Complexes.* The fluorimetric titration is an indirect method based on the competition between a fluorescent probe and a nonfluorescent competitor, both compounds forming association complexes with the $\beta$CD cavities. The used probe (4-amino-*N*-*tert*-butylphthalimide) presents a fluorescence intensity which largely increases upon $\beta$CD complexation. Adding the competitor (in this work, Ada1 or Ada2) into the solution of probe/poly$\beta$CD leads to a decrease of the fluorescence intensity of the probe. This decrease is due to the dissociation of the fluorescent (probe/poly$\beta$CD) complex by formation of a complex between the competitor and poly$\beta$CD. Assuming 1:1 inclusion complexes, the following equilibriums can be written

$$\text{probe} + \text{poly}\beta\text{CD} \leftrightarrows \text{probe/poly}\beta\text{CD} \quad \text{with} \quad K_{\text{probe}} = \frac{[\text{probe/poly}\beta\text{CD}]}{[\text{probe}][\text{poly}\beta\text{CD}]} \tag{1}$$

$$\text{Ada} + \text{poly}\beta\text{CD} \leftrightarrows \text{Ada/poly}\beta\text{CD} \quad \text{with} \quad K_{\text{Ada}} = \frac{[\text{Ada/poly}\beta\text{CD}]}{[\text{Ada}]\,[\text{poly}\beta\text{CD}]} \tag{2}$$

Note that, in writing equilibriums (1) and (2), it is implicitly assumed that the different CDs of a poly$\beta$CD chain behave independently upon complexation with the probe and the competitor. A first experiment is done with samples containing only poly$\beta$CD and probe. The fluorescence intensity variations as a function of the poly$\beta$CD concentration allow determining the complex concentration, [probe/poly$\beta$CD], and therefore $K_{\text{probe}}$.[31,33] One obtains $K_{\text{probe}} = 5900$ M$^{-1}$. From this value and the fluorescence intensity variations obtained by adding Ada1 or Ada2 into a probe/poly$\beta$CD solution, the [poly$\beta$CD] and [Ada/poly$\beta$CD] concentrations may be calculated. $K_{\text{Ada}}$ is derived as the slope of the line

$$\frac{[\text{Ada/poly}\beta\text{CD}]}{[\text{poly}\beta\text{CD}]} = K_{\text{Ada}}([\text{Ada}]_{\text{tot}} - [\text{Ada/poly}\beta\text{CD}]) \tag{3}$$

where $[\text{Ada}]_{\text{tot}}$ is the total concentration of competitor. Figure 2 shows the results obtained for a mixture involving $5.2 \times 10^{-5}$ M of probe and $5 \times 10^{-4}$ M of poly$\beta$CD cavities in the case of Ada1 and Ada2. The same experiments have also been performed using $\beta$-cyclodextrin instead of poly$\beta$CD. The results, reported in Table 1, show that Ada2 has a much higher affinity for $\beta$-cyclodextrin than Ada1. The charge, $N(CH_3)_3^+$ group, is close to the adamantyl group in Ada1 and restricts its entrance in the cavity, whereas two carbons are spacing the charge and the adamantyl group in the case of Ada2. Complexations with polymers of $\beta$-cyclodextrin lead to much lower values than in the case of the monomers, either for Ada1 and Ada2. This should be related to the electrostatic repulsions between the ligands already complexed on the chains and the incoming ligands. These electrostatic repulsions oppose the attractive inclusion complex interactions between the adamantyl moieties and the $\beta$-cyclodextrin cavities, leading to a decrease of the complexation constants by 1−2 orders of magnitude. This behavior has already been observed in the study of the complexation of poly$\beta$CD with a cationic surfactant dodecyl trimethylammonium chloride (DTAC).[33] When the electrostatic repulsions are partially screened, by adding salt in the solution, the affinity constants increase as shown by the result obtained in $10^{-2}$ M NaCl (Table 1).

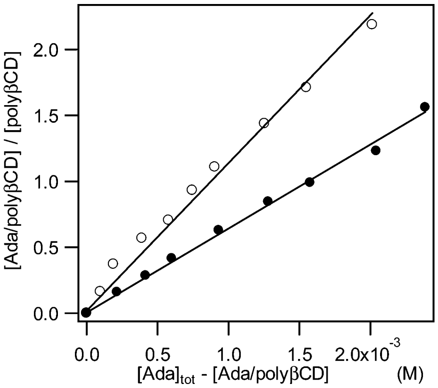

**Figure 2.** Determination of the poly$\beta$CD/Ada association constant using competitive complexation from a fluorescent probe. [Ada/poly$\beta$CD] and [poly$\beta$CD] are calculated from the fluorescent intensity measurements. The complexation constants are the linear slope (Ada1 (●) and Ada2 (○)).

**Table 1.** Complexation Constants of Ada1 and Ada2 with $\beta$-cyclodextrin Derivatives

| $\beta$-cyclodextrin derivative | $K_{\text{probe}}$ (M$^{-1}$) | $K_{\text{Ada1}}$ (M$^{-1}$) | $K_{\text{Ada2}}$ (M$^{-1}$) | $K_{\text{Ada2}}$ (M$^{-1}$) $10^{-2}$ M NaCl |
|---|---|---|---|---|
| $\beta$CD | 3100 | 6000 | 90 000 | |
| poly$\beta$CD | 5900 | 600 | 1100 | 1650 |

Nevertheless, using the complexation constants reported on Table 1, it is possible to estimate that 75 to 95% of Ada is complexed in the range of poly$\beta$CD concentrations ($5-23 \times 10^{-3}$ M) used in the following parts.

*1.2. Viscometric Results.* The reduced viscosity of a sample is defined as

$$\eta_{\text{red}} = \frac{\eta_{\text{spe}}}{C_{\text{tot}}} = \frac{\eta - \eta_0}{\eta_0 C_{\text{tot}}} \tag{4}$$

where $C_{\text{tot}}$ is the total concentration in g L$^{-1}$. Figure 3a shows the reduced viscosity of poly$\beta$CD/Ada mixtures in a 2.3 ratio of $\beta$-cyclodextrin cavity and adamantane derivative concentrations ([poly$\beta$CD]/[Ada] = 2.3) as a function of poly$\beta$CD concentration. The two binary complexes behave quite differently. The poly$\beta$CD/Ada2 reduced viscosity increases with decreasing poly$\beta$CD concentration (or else with dilution), which is typical of a polyelectrolyte behavior. This indicates that the inclusion complexes formation between Ada2 and poly$\beta$CD leads to a polycation. The poly$\beta$CD/Ada1 solution shows a behavior typical of a neutral polymer (as reported for poly$\beta$CD alone,[34] decrease of $\eta_{\text{red}}$ with dilution). Even in a different ratio ([poly$\beta$CD]/[Ada1] = 1), the poly$\beta$CD/Ada1 complex still shows the same behavior. The fluorimetric measurements (see above) have shown that Ada1 has a non-negligible affinity for the CD cavities of poly$\beta$CD, more than 70% of Ada1 being complexed in the conditions of the viscosity measurements. The unexpected viscosity behavior should be attributed to a counterion condensation occurring with the I$^-$ polarizable anions.

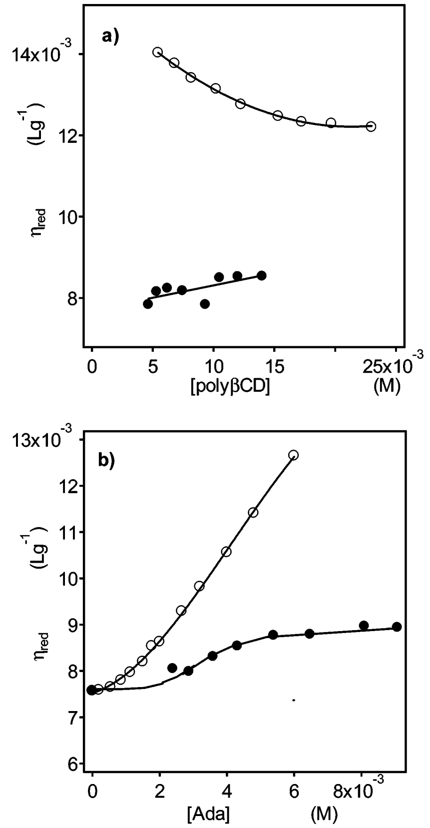

**Figure 3.** (a) Reduced viscosity as a function of $\beta$-cyclodextrin cavity concentration for poly$\beta$CD/Ada1 (●) and poly$\beta$CD/Ada2 (○) with a ratio [poly$\beta$CD]/[Ada] equal to 2.3; (b) Reduced viscosity as a function of Ada1 (●) and Ada2 (○) concentration for poly$\beta$CD/Ada mixtures with [poly$\beta$CD] = 14 × $10^{-3}$ M

In the case of Ada2, the $Br^-$ counterions are less prone to a condensation effect.[35]

The effect of Ada concentration on the reduced viscosity of poly$\beta$CD/Ada mixtures, where the molar concentration of $\beta$CD cavities is fixed at 14 × $10^{-3}$ M, is presented in Figure 3b. In general, the higher the Ada concentration in the mixture, the higher the reduced viscosity. This is what is almost observed for Ada2 for which $\eta_{red}$ progressively increases (by a factor 1.7) with increasing Ada2 concentration till 6 × $10^{-3}$ M. In fact, there are two regimes in the variations of the reduced viscosities: at low Ada2 concentration, $\eta_{red}$ is approximately constant, whereas at Ada2 concentration larger than 1.5 × $10^{-3}$ M, it increases almost linearly. In the case of the binary system poly$\beta$CD/DTAC,[34] similar behaviors have been observed and have been attributed to an inhomogeneous complexation at low DTAC concentration: the surfactant molecules are complexed at the periphery of the branched architecture of poly$\beta$CD, resulting in a negligible swelling of the chains. At larger DTAC concentrations, the surfactant molecules are more homogeneously distributed, and the electrostatic repulsions between them explain the swelling of the coils. In the case of Ada1, the results are qualitatively similar at Ada1 concentration lower than 6 mM but are more scattered due to the lower sensitivity to the Ada1 concentration. A saturation appears at larger Ada1 concentration. The origin of this effect will be discussed in the SANS part.

Figure 4a shows the reduced viscosity of NaDxS/Ada mixtures in a 2.3 ratio of sulfate group and adamantane derivative concentrations ([NaDxS]/[Ada] = 2.3) as a function of sulfate group concentration. At this ratio, the charges of the NaDxS chains are not neutralized. Thereby, the two systems still behave like polyelectrolyte chains although in a more compact conformation than in the free case as shown by the reduced viscosities which are two times lower than for free NaDxS. The binary complexes NaDxS/Ada are soluble contrary to the system NaDxS/DTAC studied in a previous work.[34] In this case, coupled hydrophobic and electrostatic interactions result in compact structures corresponding to a wrapping of the micellar domain by the NaDxS chains. The adamantyl amphiphiles do not show the same tendency to self-organize into hydrophobic microdomains as the alkyl amphiphiles. This explains partly their larger solubility. Figure 4a also reports the reduced viscosity of NaDxS/Ada1 mixture in a 1/1 ratio. Even at the charge neutralization, the system slightly behaves as a polyelectrolyte. In fact, this is certainly due to the steric hindrance of the adamantyl group. The NaDxS chain presents an average of two sulfate groups by dextran unit and the unit size is around 5 Å. An adamantyl group has a size around 7 Å; therefore, it will be difficult to bind more than one adamantane derivative per dextran unit.

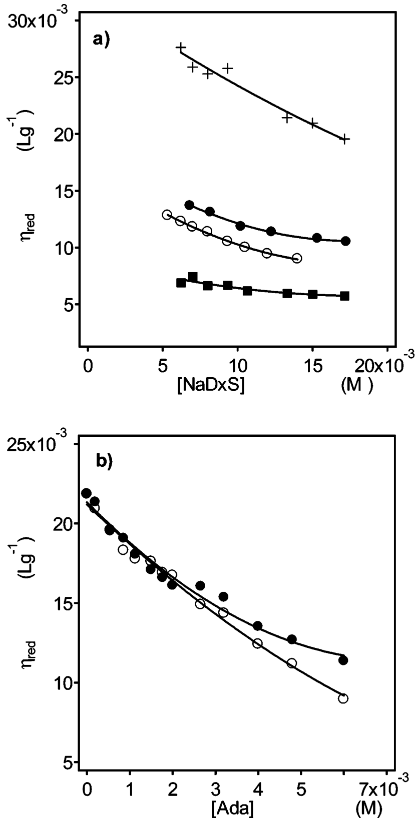

**Figure 4.** (a) Reduced viscosity as a function of sulfate group concentration for NaDxS (+), and for the mixtures NaDxS/Ada1 (●) and NaDxS/Ada2 (○) with a ratio [NaDxS]/[Ada] equal to 2.3 and NaDxS/Ada1 (■) with a ratio [NaDxS]/[Ada] equal to 1; (b) Reduced viscosity as a function of Ada1 (●) and Ada2 (○) concentration for NaDxS/Ada mixtures with [NaDxS] = 14 × $10^{-3}$ M.

The effect of Ada concentration on the reduced viscosity of NaDxS/Ada mixtures, where the molar concentration of sulfate groups is 14 × $10^{-3}$ M, is presented in Figure 4b. The reduced viscosity decreases by increasing the Ada concentration, bearing out the association of the adamantyl derivatives with NaDxS. This decreases the total charge of the chains, leading to less expended chains and consequently lower reduced viscosities.

*1.3. SANS Results—Study of the polyβCD/Ada2 Complexes.* In the first SANS experiments, a fixed cyclodextrin polymer concentration (14 mM) has been used to characterize the system in order to study the influence of Ada2 cation concentration.

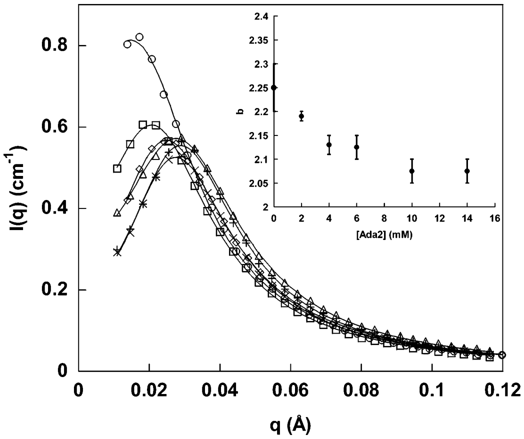

**Figure 5.** Variation of SANS scattered intensity *I*(*q*), plotted versus the scattering vector *q*, for the poly$\beta$CD/Ada2 complexes with different Ada2 concentration in $D_2O$: (○) poly$\beta$CD/Ada2 (14/1), (□) poly$\beta$CD/Ada2 (14/2), (◇) poly$\beta$CD/Ada2 (14/4), (x) poly$\beta$CD/Ada2 (14/6), (+) poly$\beta$CD/Ada2 (14/10), (△) poly$\beta$CD/Ada2 (14/14). The values of Ada2 and polymer concentration are indicated in mM. The solid lines are the result of BE fits. Inset represents the coefficient b resulting from the power law as a function of the Ada2 concentration.

The scattering behaviors of samples containing various amount of Ada2 cation ranging from 1 to 14 mM are shown in Figure 5. These results express the influence of the Ada2 addition on the conformation and interactions of the poly$\beta$CD chains. A clear diffusion peak is observed for all samples which is characteristic of a polyelectrolyte (PEL) behavior. Indeed, the observed peak indicates that, in Ada2 cation presence, poly$\beta$CD chains repulse each other by electrostatic interactions. It is important to note that the scattering intensity by Ada2 solution in $D_2O$ at 14 mM (4.2 g/L) is too weak to be detected. Thus, the PEL peak is due to the electrostatic repulsions of the complexed Ada2 cationic charge on the poly$\beta$CD chains. These results give another proof of the effective inclusion complexation between the Ada2 cations and the cyclodextrin cavities of the poly$\beta$CD at any concentration yielding a "polycation". The shape of the PEL peak is well defined for [Ada2] $\geq$ 2 mM.

The data were analyzed under the framework of the Borue Erukhimovich (BE) model[36−39] using the random phase approximation (RPA) formalism. The BE model modelized the polyelectrolyte solution as a three-component system composed of the solvent, the macroions, and the counterions. The calculated structure factor is given by

$$S(x) = C_1 \frac{(x^2 + s)}{(x^2 + s)(x^2 + t) + 1} \tag{5}$$

where $C_1$ is a scaling constant and $t$ and $s$ are the reduced temperature and the reduced charge concentration. The reduced scattering vector $x$ is given by

$$x = r_0 q \tag{6}$$

where $r_0$ is a characteristic scale of Coulombic interactions, defined as follows:

$$r_0 = a\left(\frac{48\pi l_B}{a}\phi\alpha^2\right)^{-1/4} \tag{7}$$

$a$ is the segment length, $\alpha$ is the degree of ionization, $l_B$ is the Bjerrum length, and $\phi$ is the polymer volume fraction.

The reduced charge concentration $s$ is defined in terms of the Debye screening length ($\kappa^{-1}$) and given by

$$s = \kappa^2 r_0^{\,2} \tag{8}$$

The reduced temperature $t$ stands for the solvent quality as follows:

$$t = 12\left(\frac{r_0}{a}\right)^2\left[(1 - 2\chi) + \left(\frac{3B_3}{a^3}\right)\phi\right] \tag{9}$$

$t > 0$ in good solvent and $t < 0$ in poor solvent. $B_3$ is the third virial coefficient, and $\chi$ is the Flory interaction parameter.

For $r_0^{-1} > \kappa$, eq 1 predicts the scattering maximum $q^*$ equal to

$$q^* = (r_0^{\,-2} - \kappa^2)^{1/2} \tag{10}$$

For $r_0^{-1} \ll \kappa$ or $s \gg 1$, the screening due to the salt ions becomes preponderant, and the BE model is not valid. In this case, the structure factor is similar to ones obtained for neutral polymer solutions.

The solid lines of Figure 5 show the results of the BE fits to the data using eq 5 with $C_1$, $s$, $t$, and $r_0$ as adjustable parameters. The BE model fits quite well the data, and the adjustable and deduced parameters are displayed in Table 2. The degree of ionization $\alpha$ is calculated in a first approximation assuming a total complexation of Ada2; that is, $\alpha$ is equal to the molar ratio between the cation charge and cyclodextrin cavity.

It is verified that $r_0^{-1} > \kappa$ for all of the samples. To find the peak position independently of any model, we used a polynomial fitting through few points around the scattered intensity maximum, and the corresponding calculated position is noted $q^*_{\text{calc}}$. This calculated peak position is compared to the peak position $q^*_{\text{BE}}$ from eq 10 as shown in Table 2. There is a good correlation between $q^*_{\text{calc}}$ and $q^*_{\text{BE}}$, showing that the BE model adequately represents our data. The position of the peak $q^*$ is shifted toward higher $q$ values (see Table 2) when the charge concentration is increased due to the increased polyelectrolyte contribution to the whole signal. The peak position reaches a constant value at [Ada2] larger than 6 mM, due to a compensation in eq 10 of $r_0^{-2}$ and $\kappa^2$ increases.

The BE model allows to have access to the segment length $a$ provided by eqs 7 and 10 and given by

$$r_0^{\,-2} = q^{*2} + \kappa^2 = [a^{-5/2}(48\pi l_B)^{1/2}]\alpha\phi^{1/2} \tag{11}$$

A linear fit of $r_0^{-2}$ versus $\alpha\phi^{1/2}$ should enable the determination of the segment length $a$. The parameters of eq 11 were calculated independently of the previous BE fits: $q^*$ is the $q^*_{\text{calc}}$, $\alpha$ is the calculated ionization degree, the polymer volume fraction $\phi$ is equal to 0.018, and $\kappa$ is estimated by $\kappa^2 = 8\pi l_B I \aleph$, where $I$ is the ionic strength and $\aleph$ is the Avogadro number. The ionic strength is attributed to the Ada2 counterions: $I =$ [Ada2] /2. The results are presented in Figure 6. The slope of the linear fit provides a segment length $a = 18$ Å. This value is in good agreement with our expectations since the $\beta$-cyclodextrin size is 15 Å and several hydroxypropyl units connect the different cavities. However, it is seen that the linear fit cannot cover the whole range of data but can only be applied at an ionization degree lower than 0.5. Although the departure from linearity corresponds to only three data points, one can discuss the validity of the BE model in this range: it has been developed

**Table 2.** Adjustable ($C_1$, $r_0$, $s$, and $t$), Deduced ($q^*_{BE}$) and Calculated ($\alpha$, $q^*_{calc}$) Parameters Based on BE Theory for the Binary Systems Poly$\beta$CD/Ada2

| complexes | [Ada2] (mM) | $\alpha$ | $C_1$ | $r_0$ (Å) | $s$ | $t$ | $q^*_{BE}$ (Å$^{-1}$) | $q^*_{calc}$ (Å$^{-1}$) |
|---|---|---|---|---|---|---|---|---|
| poly$\beta$CD/Ada2 14/1 | 1 | 0.07 | 0.803 | 37.187 | 0.698 | −0.315 | 0.01479 | 0.01624 |
| poly$\beta$CD/Ada2 14/2 | 2 | 0.14 | 0.628 | 34.512 | 0.489 | −0.473 | 0.02071 | 0.02047 |
| poly$\beta$CD/Ada2 14/4 | 4 | 0.28 | 0.595 | 32.042 | 0.362 | −0.590 | 0.02492 | 0.02548 |
| poly$\beta$CD/Ada2 14/6 | 6 | 0.43 | 0.469 | 29.889 | 0.323 | −0.786 | 0.02753 | 0.02795 |
| poly$\beta$CD/Ada2 14/10 | 10 | 0.71 | 0.438 | 28.036 | 0.343 | −0.867 | 0.02891 | 0.02969 |
| poly$\beta$CD/Ada2 14/14 | 14 | 1 | 0.433 | 26.538 | 0.464 | −0.771 | 0.02758 | 0.02818 |

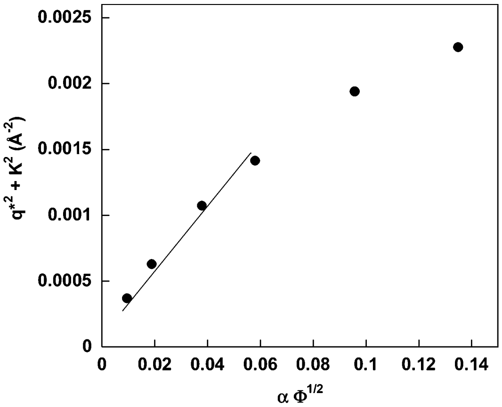

**Figure 6.** Variation of the peak position with the ionization degree of the complexes. The polymer volume fraction is fixed at $\phi = 0.018$ ([poly$\beta$CD]=14 mM).

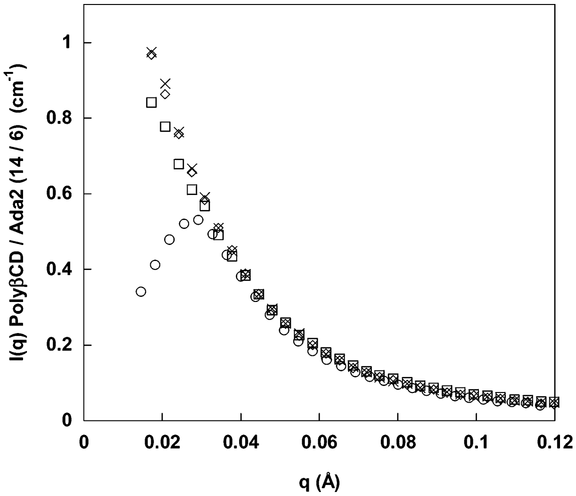

**Figure 7.** Effect of added salt: (○) 0 salt-free, (□) 15, (◇) 150, (x) 500 mM. Variation of the SANS intensity $I(q)$ as a funtion of $q$ for poly$\beta$CD/Ada2 (14/6) system at different added salt concentrations [NaCl].

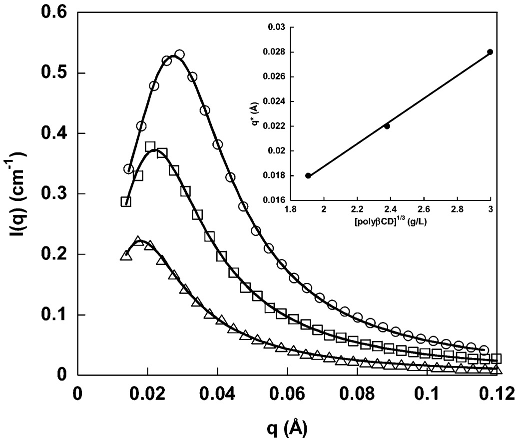

**Figure 8.** Effect of cyclodextrin polymer concentration [poly$\beta$CD]. Variation of SANS intensity $I(q)$, plotted versus the scattering vector $q$, for the poly$\beta$CD/Ada2 complexes (○) (14/6), (□) (7/3), (△) (3.5/1.5) in $D_2O$. The solid lines are the result of the BE fit. Inset represents the variations of the PEL peak position as a function of poly$\beta$CD concentration.

for linear polyelectrolytes, whereas the poly$\beta$CD has the constraint of a branched architecture and is not able to swell as highly charged polyelectrolytes.

Information about the internal structure of the polymer complex can be obtained by analyzing the asymptotic behavior of the scattering intensity $I(q)$ at large $q$ values. Thus, $I(q)$ in this $q$ domain is represented by a power law $I(q) \propto q^{-b}$. Theoretically, the more compact the scattering bodies, the higher the $b$ values: $b = 1$ is expected for a rigid rod, $b = 2$ for an ideal chain, and $b = 4$ for a collapsed chain.[40,41] For poly$\beta$CD alone in solution, $b = 2.25$, a value close to the one predicted by Daoud and Joanny in a Flory model of randomly branched polymers in theta solvent conditions (2.28).[42] For the binary mixtures poly$\beta$CD/Ada2, the $b$ exponents slightly decrease with the Ada2 concentration, as shown in the inset of the Figure 5: $b = 2.07$ for [Ada2] $= 14 \times 10^{-3}$ M. The radius of the polymer complex is expected to vary as $N^{1/b}$ where $N$ is the average number of cyclodextrins per chain ($N = 83$). The swelling ratio of the mixture containing [Ada2] $= 6 \times 10^{-3}$ M ($b = 2.12$) compared to pure poly$\beta$CD ($b = 2.25$) can thus be calculated using the following relationship: $N^{3/2.12\ -\ 3/2.25}$. This gives a swelling ratio of 1.4, which is in good agreement with the viscosity results presented on Figure 3b: the swelling ratio 1.6 is estimated from the ratio of the reduced viscosities.

*1.3.1. Effect of Salt Concentration.* The variation of the SANS scattering intensity $I(q)$ as a function of $q$ at different added salt concentration [NaCl] of the system poly$\beta$CD/Ada2 (14/6) is reported in Figure 7. The added salt concentrations are [NaCl] = 0 (salt-free), 15, 150, and 500 mM. Upon a small addition of salt (15 mM), the PEL peak in salt-free condition disappears, replaced by a monotonic intensity decrease as a function of $q$. The same behavior is also observed at higher salt concentration. Thus, an addition of a simple electrolyte (NaCl) results in a scattering behavior closer to that of a neutral polymer. The explanation of this effect is based on the electrostatic nature of the peak. Indeed, a progressive screening of long-range electrostatic forces is observed when [NaCl] increases and a neutral behavior is eventually reached. Repulsive interactions have been completely screened at [NaCl] = 150 mM, and diffusion spectra are superimposed for larger salt concentrations. In this system, above 150 mM of salt, poly$\beta$CD/Ada2 chains behave as neutral chains and the chain structures are independent of the ionic strength.

*1.3.2. Effect of Polymer Concentration.* It is seen from Figure 8 and the obtained values of $q^*_{BE}$ based on BE theory reported in Table 3 that the PEL peak position moves toward higher $q$ values with increasing polymer concentration. This behavior

**Table 3.** Influence of Dilution on the PEL Peak Position Based on BE Theory

| $C_{\text{poly}\beta\text{CD}}$ (mM) | [Ada2] (mM) | $q^*_{\text{BE}}$ (Å$^{-1}$) |
|---|---|---|
| 3.5 | 1.5 | 0.01809 |
| 7 | 3 | 0.02205 |
| 14 | 6 | 0.02753 |

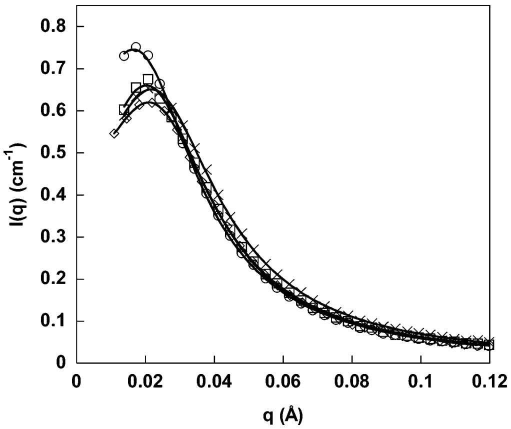

**Figure 9.** Variation of SANS scattered intensity *I*(*q*), plotted versus the scattering vector *q*, for the poly*β*CD/Ada1 complexes with Ada1 concentration (○) poly*β*CD/Ada1 (14/2), (□) poly*β*CD/Ada1(14/4), (◇) poly*β*CD/Ada1 (14/6), (x) poly*β*CD/Ada1 (14/10) in $D_2O$. The values of Ada1 and polymer concentration are indicated in mM. The solid lines are the result of the BE fit.

indicates a decrease of the characteristic scale of Coulombic interaction by progressive screening of long-range repulsions, i.e., counterion concentration increase with [Ada2]. Interestingly, the BE model was not successful to predict the variations of $q^*$ as a function of the polymer concentration: $q^{*2} + \kappa^2$ does not vary proportionally to $\alpha\phi^{1/2}$ when $\phi$ is varied. As already mentioned, the poly*β*CD polymer has a branched architecture, which could explain this discrepancy. The best fit corresponds to a linear relationship between $q^*$ and $\phi^{1/3}$ like it is represented in the inset of Figure 8. The long-range electrostatic interactions impose a preferential distance between charged particles and lead to an "organized structure" characteristic of a cubic arrangement $q^* \propto [\text{poly}\beta\text{CD}]^{1/3}$in the dilute regime. Similar $q^*$ variations have been observed on micellar aggregates of amphiphilic diblock polyelectrolytes,[43] charged dendrimers,[44−46] and charged arborescent graft polymers.[47] Conformations of branched polyelectrolytes have been studied theoretically.[48,49] Interaction models based on charged soft spheres[49,50] are in agreement with the experimental results based on the concentration influence.

*1.4. SANS Results−Study of the PolyβCD/Ada1 Complexes.* To study the effect of the cation nature on the cyclodextrin polymer, experiments have been performed with the cation Ada1. Figure 9 shows the Ada1 cation concentration influence on the scattering diffusion spectra for the mixtures poly*β*CD/Ada1 containing various amounts of Ada1 ranging from 2 to 10 mM and a fixed poly*β*CD concentration at [poly*β*CD] = 14 mM. These results show a polyelectrolyte behavior by the appearance of a correlation peak due to the electrostatic repulsions between Ada1 and the poly*β*CD chains. At [Ada1] ≥ 4 mM, all of the diffusion peaks are almost superimposed, and the peak maximum remains unaltered by increasing the Ada1 concentration. Indeed, from the BE parameter fits compiled in Table 4, there are negligible variations in the PEL peak position $q^*$. The previous fluorimetric titration experiment has shown that Ada1 has a lower affinity for poly*β*CD ($K_{\text{Ada1}} = 600$ M$^{-1}$) than Ada2 but in the conditions of the SANS experiments a large majority of the cations are making inclusion complexes: for instance, at [Ada1] = 6 mM, 85% of the cations are complexed. On the contrary, the viscosity results show much lower expansions of the coils when Ada1 is added than with Ada2 (Figure 3b). This can be attributed to larger counterion condensations ($I^-$) in the case of Ada1. In this frame, the SANS results can be explained by a constant effective charge of the decorated poly*β*CD chains when [Ada1] is larger than 4 mM.

We have also analyzed the asymptotic behavior at larger *q* values $I(q) \propto q^{-b}$ for all of the samples ranging from 2 to 10 mM in Ada1 concentration. As was observed for Ada2, the cation linking induces a slight decrease of the exponents *b*, from $b = 2.05$ ([Ada1] = 2 mM) to $b = 1.98$ ([Ada1] = 10 mM).

**2. Ternary Complexes.** Ada1 and Ada2 interact both with poly*β*CD and NaDxS by inclusion complexation and electrostatic interactions, respectively. In the following section, we will report results regarding the ternary complexes poly*β*CD/Ada/NaDxS.

*2.1. Viscometric Results.* Viscometry was first chosen to prove the formation of ternary complexes for particular soluble mixtures in water, with the same concentrations ratio as in previous works.[33,34] The concentrations ratio is 2.3 both for the *β*-cyclodextrin cavity/adamantane derivative and for the sulfate group/adamantane derivative. Figure 10a shows the reduced viscosity of poly*β*CD/Ada1/NaDxS and poly*β*CD/Ada2/NaDxS as a function of poly*β*CD concentration (or sulfate group concentration). The observed reduced viscosity decreases with dilution, typical of a neutral polymer behavior. The binary systems poly*β*CD/Ada and Ada/NaDxS, whose reduced viscosities are shown in Figures 3a and 4a, do not show the same trend. The reduced viscosities of the ternary mixtures could not be fitted assuming ideal mixtures of the binary systems. Indeed, there are additional interactions that are to be taken into account which screen the electrostatic interactions due to the polyelectrolytes. This occurs through the formation of ternary complexes, involving electrostatic attractive interactions between Ada and NaDxS and inclusion complexes between Ada and poly*β*CD. Moreover, the values of the reduced viscosity of the poly*β*CD/Ada2/NaDxS ternary complex are lower than those of the two binary complexes, poly*β*CD/Ada2 and NaDxS/Ada2, suggesting aggregates with compact structures.

The effect of Ada concentration on the reduced viscosity of poly*β*CD/Ada/NaDxS mixtures, where the molar concentration of *β*CD cavities and of sulfate groups is $14 \times 10^{-3}$ M, is presented in Figure 10b. In the case of Ada1, the reduced viscosity increases slightly with the Ada1 concentration, which indicates the formation of larger aggregates. Above [Ada1] = $1.5 \times 10^{-3}$ M, the reduced viscosity decreases only slightly. Larger variations are observed for Ada2. The reduced viscosity decreases slightly until the same critical concentration as for [Ada1] = 1.5 $10^{-3}$ M and then a stronger decrease takes place indicating the formation of denser and denser aggregates up to their precipitation at [Ada2] > $6 \times 10^{-3}$ M. A similar behavior was observed for the system poly*β*CD/DTAC/NaDxS,[34] where a critical concentration was also observed around $1.5 \times 10^{-3}$ M for which a structural transition was proposed for both the binary poly*β*CD/DTAC and the ternary complexes. At low cation concentration, the DTAC decorated poly*β*CD chains are weakly charged, and the charges are distributed on an outer corona of the polymer coil.[51] Their weak attraction for the NaDxS chains does not lead to compact structures, the NaDxS chains being still swollen in the corona. As the cation

**Table 4.** Adjustable ($C_1$, $r_0$, $s$, and $t$), Deduced ($q^*_{BE}$) and Calculated (α, $q^*_{calc}$) Parameters Based on BE Theory for the Binary System Poly$\beta$CD/Ada1

| complexes | [Ada1] mM | α | $C_1$ | $r_0$ (Å) | $s$ | $t$ | $q^*_{BE}$ (Å$^{-1}$) | $q^*_{calc}$ (Å$^{-1}$) |
|---|---|---|---|---|---|---|---|---|
| poly$\beta$CD/Ada1 14/2 | 2 | 0.14 | 0.794 | 36.657 | 0.631 | −0.305 | 0.01658 | 0.01709 |
| poly$\beta$CD/Ada1 14/4 | 4 | 0.28 | 0.717 | 34.29 | 0.517 | −0.399 | 0.02028 | 0.02015 |
| poly$\beta$CD/Ada1 14/6 | 6 | 0.43 | 0.476 | 29.289 | 0.622 | −0.610 | 0.02099 | 0.02056 |
| poly$\beta$CD/Ada1 14/10 | 10 | 0.71 | 0.630 | 30.653 | 0.556 | −0.477 | 0.02173 | 0.02127 |

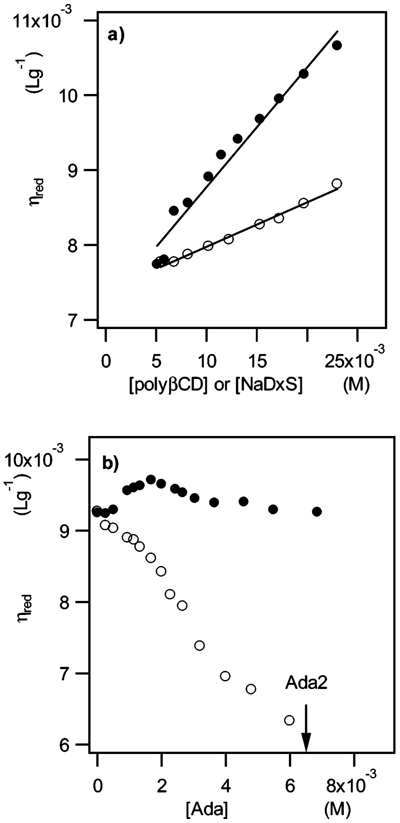

**Figure 10.** (a) Reduced viscosity as a function of poly$\beta$CD or NaDxS concentration for poly$\beta$CD/Ada1/NaDxS (●) and poly$\beta$CD/Ada2/NaDxS (○) mixtures b) Reduced viscosity as a function of [Ada] concentration for poly$\beta$CD/Ada1/NaDxS (●) and poly$\beta$CD/Ada2/NaDxS (○) mixtures with [poly$\beta$CD] = [NaDxS] = 14 × $10^{-3}$ M. The arrow indicates the Ada2 concentration at which the system phase-separates

concentration is larger than the critical value, the charges start to be distributed homogeneously along the poly$\beta$CD coil, and the attractions for the NaDxS chains are stronger, leading to a gradual deswelling of the NaDxS chains belonging to the complexes. Moreover, the previous studies have shown that the NaDxS chains are too large to penetrate into the branched structure of the poly$\beta$CD chains but rather wrap around them. This model holds also for the Ada ternary systems. For Ada 2, the weak viscosity decrease corresponds to the first regime ([Ada2] < 1.5 mM). At larger Ada2 concentration, the strong viscosity decrease is due to the large attraction between the poly$\beta$CD and the NaDxS chains, inducing the formation of compact aggregates of increasing molecular weight. Phase separation should occur when the aggregates start to overlap.

In the case of Ada1, the very low viscosity decrease can be attributed to a larger counterion condensation than for Ada2. Indeed, the cations buried in the center of the poly$\beta$CD coil do not interact directly with the NaDxS (located on the outer corona). Counterion condensation with the $I^-$ soft anions should be favored, decreasing the strength of the interaction with the polyanions and thus explaining the low viscosity effects.[35]

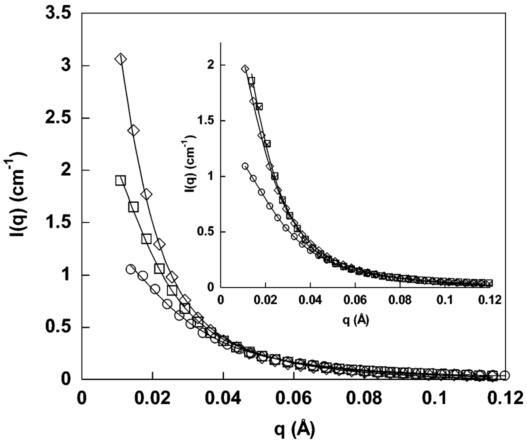

**Figure 11.** Scattered intensities of the ternary systems: (○) poly$\beta$CD/Ada2/NaDxS (14/1/14), (□) poly$\beta$CD/Ada2/NaDxS (14/2/14), (◇) poly$\beta$CD/Ada2/NaDxS (14/4/14). Inset represents the scattered intensities of Ada1 system (○) poly$\beta$CD/Ada1/NaDxS (14/2/14), (□) poly$\beta$CD/Ada1/NaDxS (14/4/14), (◇) poly$\beta$CD/Ada1/ NaDxS (14/6/14), (+) poly$\beta$CD/Ada1/NaDxS (14/10/14). Solid lines fit the curves based on Debye function.

*2.2. SANS Results.* Previous work has shown that, although NaDxS is a PEL, no diffusion peak by NaDxS alone is observed meaning that in the concentration range of the experiments, its scattering intensity is too weak to be detected. Thus, the data may be interpreted in terms of scattering by poly$\beta$CD or by its complexes only.

When the ternary system poly$\beta$CD/Ada2/NaDxS is formed, the PEL peak in the scattering intensity of poly$\beta$CD/Ada2 disappears which indicates a screening of Coulombic repulsive interactions of polycationic chains (Figure 11). This is due to the interaction of opposite charges between the negative charges of NaDxS and the positive charges of poly$\beta$CD/Ada2.

In a similar way as was done for binary systems, the internal structure of the system is obtained by the asymptotic behavior of $I(q)$ at large $q$ values by the power law $I(q) \propto q^{-b}$. These ternary systems show a $q^{-2}$ dependence of the scattered intensity, $b$ being insensitive to the charge ratio. These results seem to be in contradiction with the viscosity ones (see Figure 10b), which show a large sensitivity to the charge ratio. It should be recalled that the asymptotic large $q$ scattering behavior check the internal structure of the aggregates whereas the viscosity measurements are indicative of the compacities of the whole aggregates. Moreover, aggregates with an inhomogeneous distribution of the two polymers, a core−shell-structure for instance (the core being composed of poly$\beta$CD and the shell of a NaDxS layer), should display an apparent power law, which corresponds to a combination of the scattering from the core and from the shell. Increasing the Ada2 concentration should induce a slight expansion of the poly$\beta$CD core (due to its increased charge density), whereas the NaDxS shell should be more compact (due to an increased attraction to the core). The negligible sensitivity of the apparent $b$ exponent to the charge ratio reflects thus the combination of two opposite effects and is not in contradiction with the viscosity measurements.

**Table 5.** Values of the Radius of Gyration Estimated by the Debye Function Fits of Ternary Complexes

| concentration | poly$\beta$CD/Ada/NaDxS | | | | |
|---|---|---|---|---|---|
| ratio | 14/1/14 | 14/2/14 | 14/4/14 | 14/6/14 | 14/10/14 |
| Rg Ada1 (Å) | | 62 | 90 | 82 | 88 |
| Rg Ada2 (Å) | 63 | 83 | 107 | NA | NA |

As shown on Figure 11, the scattered intensities decrease monotonically as a function of $q$ for all of the ternary mixtures, reflecting negligible repulsive interaction potentials between them. This proves that the complexes are almost neutral and that they do not experience hard core interaction potentials. Due to low contrast in the scattering length densities of poly$\beta$CD and NaDxS, it has not been possible to perform contrast-matching experiments to deduce information about poly$\beta$CD distribution in the complexes. To characterize the structure of the complexes, and taking into account the results at large $q$, an attempt was done to fit the scattering profile of the ternary system as the one of an ideal chain. Indeed, the SANS intensity patterns $I(q)$ show a monotonically decrease similar to neutral polymer solutions. The $R_g$ averaged structure was estimated from the scattering curves by Debye function[37,52] fits based on the formula

$$I(q) = A + \left(\frac{B}{x^2}\right)(e^{-x} - 1 + x) \qquad (12)$$

where $x = q^2R_g{}^2$ and $R_g$ is the radius of giration, $A$ is an incoherent baseline parameter, and $B$ is an arbitrary intensity scaling factor. As shown in Figure 11, the Debye function fits the data quite well over the whole range of scattering angles.

The $R_g$ based on the Ada2 system ranges from 63 Å for poly$\beta$CD/Ada2/NaDxS (14/1/14) to 107 Å for poly$\beta$CD/Ada2/NaDxS (14/6/14). The increase is due to the ability of the system to bind more NaDxS resulting in the biggest structures. Aggregates whose core is formed by one poly$\beta$CD chain may thus be formed. No measurement at Ada2 concentration higher than 6 mM is available because of the precipitation of the system. It has been calculated that, on average, single poly$\beta$CD chains have a 300 Å center-to-center distance when in solution in the concentration of the experiments (14 mM). Thus, when the radius of the complex is larger than half this critical distance, the different complexes may interact one with each other and lead to precipitation due to a bridging effect (NaDxS chains can link several poly$\beta$CD chains). This simple calculation is in agreement with the concentration domain where precipitation is observed: at an Ada2 concentration of 6 mM, the extrapolated radius of gyration should be around 140 Å.

The experiments performed with the Ada1 ternary systems give qualitatively the same behaviors as for Ada2. The results of the nonlinear curve fitting for $R_g$ are reported in Table 5. The $R_g$ of the averaged structure based on Ada1 system increases from 62 Å for poly$\beta$CD/Ada1/NaDxS (14/2/14) and quickly reaches a limit value close to 85 Å for [Ada1] $\geq$ 4 mM. It should be noted that the radius of gyration of pure poly$\beta$CD is equal to 55 Å. As observed for the Ada2 systems, it appears that the complexes are probably built around one poly$\beta$CD chain. The limited increase of the aggregate size is in agreement with the viscosity results (Figure 10b).

## Discussion and Conclusion

The experiments of this study have shown that ternary complexes can be formed by mixing a $\beta$-cyclodextrin containing polymer (poly$\beta$CD), a dextran sulfate polyanion (NaDxS), and cationic connectors which are adamantyl derivatives (Ada1 or Ada2) in aqueous medium. These components are assembling via coupled inclusion complex interactions (adamantyl group and cyclodextrin cavity) and electrostatic attractive interactions (positive charges of Ada and negative charge of NaDxS). The study has been divided in two parts: a characterization of the binary systems before a study of the ternary ones because it was of prime importance to understand the binary interactions prior to a description of the interaction mechanism in the whole system.

The following discussion will be focused on the results of the Ada2 derivatives, the particular behavior of the Ada1 systems being discussed at the end of this part.

Each of the three possible binary systems has been considered. A previous study has shown that there was no specific interaction between poly$\beta$CD and NaDxS.[34] On the contrary, Ada derivatives link to either poly$\beta$CD or to NaDxS. Electrostatic interactions are responsive of the Ada2 to NaDxS linking, as characterized by the large viscosity reductions upon Ada2 addition. It should be mentioned that Ada2/NaDxS complexes are soluble in a large stoichiometric range, contrary to the behavior observed using a cationic surfactant like DTAC.[34,51,53] The Ada2 affinity for the cyclodextrin cavities of the poly$\beta$CD has been determined through fluorimetric experiments. The complexation constants are almost 100 times lower than the one expected for complexation into native $\beta$-cyclodextrin without added salt but increases markedly when NaCl is added to the medium. This behavior is due to the polyelectrolyte nature of the complex, with the electrostatic potential induced by the charges on the decorated poly$\beta$CD chains opposing to an increase of the Ada2 binding. However, the complexation constants are always high enough to ensure the binding of a large majority of the Ada2 molecules. Viscosity and SANS measurements show that poly$\beta$CD/Ada2 complexes behave as polyelectrolytes, with reduced viscosity increase at low concentration and correlation peaks in the neutron scattered intensities.

Mixing the three components in aqueous media results in large viscosity reductions correlated with the disappearance of the polyelectrolyte peaks in the scattered intensities and with intensity increase at low $q$. The radius of gyration of the aggregates is found to increase from 60 Å (a value close to the one of pure poly$\beta$CD) to 110 Å. The results are in good agreement with a core–shell complexation mechanism already developed for the ternary system poly$\beta$CD/DTAC/NaDxS.[51] The structure of the ternary system is reminiscent of the one of the binary system poly$\beta$CD/Ada2. The core is constituted of the poly$\beta$CD/Ada2 complex and the shell is made of NaDxS chains interacting electrostatically with the positively charged core as schematized on Figure 12. At low Ada2 concentration, the attraction is weak and the linked NaDxS are making few contacts with the surface of the core. As the Ada2 concentration is increased, the electrostatic interactions increase, leading to both increased association with NaDxS and to compaction of the shell. This model is in good agreement with the neutron scattering and viscosity results: both the molecular weight and the radius of gyration of the aggregates increase with the Ada2 concentration whereas their global compacities decrease. Moreover, this model is able to predict the solubility limit of the complexes: soluble complexes are formed until the diameters of the aggregates become comparable to their average spacing distance. Above this limit, attractive bridging interactions should occur between the aggregates leading to phase separation. It

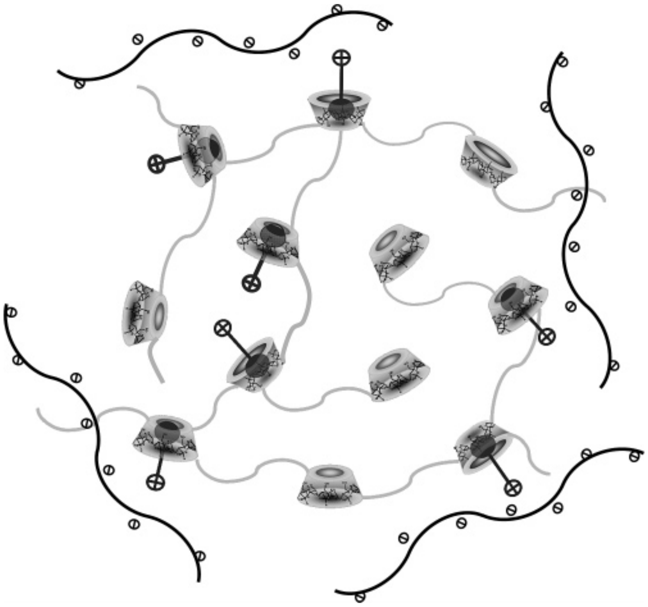

**Figure 12.** Schematic representation of the ternary complex between the poly$\beta$CD, the cation and NaDxS.

should be mentioned that attractive bridging interactions do not have to overcome strong repulsive electrostatic interactions to establish the fact that the primary aggregates have a low global charge (no polyelectrolyte peak and neutral type viscosity behavior). Then, the bridging should occur by involving a single NaDxS chain which links two poly$\beta$CD/Ada cores by interacting electrostatically between them. In the concentration range of the experiments, the Ada2 concentration for phase separation is 6 mM where the extrapolated diameter of the aggregates would be 280 Å, a value comparable to the average spacing distance between poly$\beta$CD chains (300 Å). The good correlation between these two values proves also the validity of the core–shell model where the core contains only one poly$\beta$CD chain.

Compared to the DTAC surfactants,[16] the Ada2 amphiphiles produce aggregates with a smaller size and a more compact structure under the same concentration conditions. There are structural differencies in the two cases which can be understood considering that the ternary complexes are constituted of primary aggregates with a core–shell structure, the core containing one poly$\beta$CD chain. The larger size of the DTAC aggregates can be attributed to a moderate association of the primary structures. These associations, which are only effective for the DTAC systems, could be due to a competiting self-association mechanism of DTAC. The Ada2 systems keep their primary structures because the Ada amphiphiles are not subject to self-association.

Ada1 cationic amphiphiles have given quite unexpected results. The original goal of this study was to show the influence of the charge position on the connector, a better decoupling of the electrostatic and inclusion complex interactions being expected when a spacer is introduced between the positive charge and the hydrophobic guest group. The electrostatic interactions between Ada1 and NaDxS are comparable to the ones obtained with Ada2, showing a low influence of the spacing group in this case. As expected, Ada1 has a lower affinity for poly$\beta$CD than Ada2 due to the absence of spacer in Ada1: the proximity of the charge restricts the entrance inside the cavity. However its affinity is large enough to ensure complexation of a large majority of the Ada1 under the experimental conditions of this work. Viscometry and neutron scattering results for poly$\beta$CD/Ada1 are quite different than those obtained for poly$\beta$CD/Ada2: the scattered intensities are almost insensitive to the Ada1 addition above an Ada1 concentration equal to 4 mM and the reduced viscosities show a neutral type behavior. This phenomenom is attributed to a larger counterion condensation of the $I^-$ polarizable counterion of Ada1 than the $Br^-$ counterion of Ada2 around the polyelectrolyte complexes.[35] The results can be analyzed in terms of lower effective charge densities of the poly$\beta$CD/Ada1 complex. In the case of the ternary system, the aggregates are smaller and less compact than with Ada2. This is again interpreted in terms of large $I^-$ counterion condensation, but the mechanism is more subtle. We have seen that direct electrostatic interaction can occur between Ada1 and NaDxS which are able to displace the $I^-$ counterions. In the frame of the interaction mechanism schematized in Figure 12, the Ada1 cations located at the periphery of the poly$\beta$CD core do interact directly with the NaDxS chains. This explains why at low Ada1 concentration there is the formation of ternary complexes. However, increasing the Ada1 concentration above a critical concentration (1.5–2 mM) results in a larger amount of cations located inside the poly$\beta$CD core. The electrostatic interactions generated by these ions are, for the most part, screened by $I^-$ counterion condensation. With the Ada1 cations being buried inside the poly$\beta$CD core, displacement of $I^-$ counterions by close association with the NaDxS charges is unfavorable. Thus, there is almost no further increase of the aggregation above the critical concentration, as seen from viscosity and neutron scattering results (Figures 10 and 11). This study shows that Ada1 cationic amphiphiles are less efficient than Ada2 in building large ternary complexes. This phenomenom is mostly attributed to a counterion effect than to the influence of a spacer group between the charge and the hydrophic group.

This study has allowed us to understand the interaction mechanisms in a model ternary system driven by coupled electrostatic and inclusion complex interactions. It has shown that the nature of the cationic amphiphile, at the origin of its ability to self-associate, and the nature of the counterion are playing an important role in determining the structural properties of the ternary complexes. Potential applications of these systems depend on the choice of the polyanion. Ternary complexes performed with DNA are potential gene carriers. First transfection efficiency experiments have given encouraging results which can be improved changing the nature of the poly$\beta$CD and/or of the connectors. Drug delivery with negatively charged proteins can also benefit from the versatility of such a system.

## References and Notes

(1) Pocar, I.; Sergeot, P.; Tribet, C.; Cormick, M., Ed.; ACS symposium, 2000; American Chemical Society: Washington, DC, 2000; Vol. series 780, p 82.

(2) Akiyoshi, K.; Deguchi, S.; Moriguchi, N.; Yamaguchi, S.; Sunamoto, J. *Macromolecules* **1993**, *26*, 3062–3068.

(3) Armstrong, F. A.; Wilson, G. S. *Electrochim. Acta* **2000**, *45*, 2623–2645.

(4) Fragoso, A.; Caballero, J.; Almirall, E.; Villalonga, R.; Cao, R. *Langmuir* **2002**, *18*, 5051–5054.

(5) Glass, J. E., Ed. *Polymers as rheology modifiers*, American Chemical Society: Washington, DC, 1991.

(6) Harada, A.; Kataoka, K. *Science* **1999**, *283*, 65–67.

(7) Decher, G. *Science* **1997**, *277*, 1232–1237.

(8) Myers, J.; Pace, C. *Biophys. J.* **1996**, *71*, 2033–2039.

(9) Tareste, D.; Pincet, F.; Perez, E.; Rickling, S.; Mioskowski, C.; Lebeau, L. *Biophys. J.* **2002**, *83*, 3675–3681.

(10) Okumura, H.; Okada, M.; Kawaguchi, Y.; Harada, A. *Macromolecules* **2000**, *33*, 4297–4298.

(11) Lu, J.; Mirau, P. A.; Shin, I. D.; Nojima, S.; Tonelli, A. E. *Macromol. Chem. Phys.* **2002**, *203*, 71–79.

(12) Rusa, C. C.; Luca, C.; Tonelli, A. E. *Macromolecules* **2001**, *34*, 1318–1322.

(13) Sandier, A.; Brown, W.; Mays, H.; Amiel, C. *Langmuir* **2000**, *16*, 1634−1642.
(14) Amiel, C.; Sebille, B. *Adv. Colloid Interface Sci.* **1999**, *79*, 105−122.
(15) Auzely-Velty, R.; Rinaudo, M. *Macromolecules* **2002**, *35*, 7955−7962.
(16) Islam, M. F.; Jenkins, R. D.; Bassett, D. R.; Lau, W.; Ou-Yang, H. D. *Macromolecules* **2000**, *33*, 2480−2485.
(17) Saenger, W. In *Inclusion Compounds*; Atwood, J. L., Davies, J. E. D., MacNicol, D. D., Eds.; Academic Press: London, 1984; Vol. 2.
(18) Szejtli, J. *Cyclodextrin technology*; Kluwer Academic Publishers: Dordrecht, 1988.
(19) Eftink, M. R.; Andy, M. L.; Bystrom, K.; Perlmutter, H. D.; Kristol, D. S. *J. Am. Chem. Soc.* **1989**, *111*, 6765−6772.
(20) Amiel, C.; Moine, L.; Sandier, A.; Brown, W.; David, C.; Cormick, M., Ed.; ACS symposium, 2000; American Chemical Society: Washington, DC, 2000; Vol. series 780, p 58.
(21) Weickenmeier, M.; Wenz, G. *Macromol. Rapid Commun.* **1997**, *18*, 1109−1115.
(22) Gref, R.; Amiel, C.; Molinard, K.; Daoud-Mahammed, S.; Sebille, B.; Gillet, B.; Beloeil, J.-C.; Ringard, C.; Rosilio, V.; Poupaert, J.; Couvreur, P. *J. Controlled Release* **2006**, *111*, 316−324.
(23) Pun, S. H.; Bellocq, N. C.; Liu, A.; Jensen, G.; Machemer, T.; Quijano, E.; Schuep, T.; Wen, S.; Engler, H.; Heidel, J.; Davis, M. E. *Bioconjugate Chem.* **2004**, *15*, 831−840.
(24) Arima, H.; Kihara, F.; Hirayama, F.; Uekama, K. *Bioconjugate Chem.* **2001**, *12*, 476−484.
(25) Amiel, C.; Galant, C.; Auvray, L. *Prog. Colloid Polym. Sci.* **2004**, *136*, 44−46.
(26) Burckbuchler, V.; Wintgens, V.; Lecomte, S.; Percot, A.; Leborgne, C.; Danos, O.; Kichler, A.; Amiel, C. *Biopolymers* **2006**, *81*, 360−370.
(27) Choi, H. S.; Ooya, T.; Sasaki, S.; Yui, N. *Macromolecules* **2003**, *36*, 5342−5347.
(28) Pollard, H.; Remy, J.-S.; Loussouarn, G.; Demolombe, S.; Behr, J.-P.; Escande, D. *J. Biol. Chem.* **1998**, *273*, 7507−7511.
(29) Renard, E.; Barnathan, G.; Deratani, A.; Sébille, B. *Macromol. Symp.* **1997**, *122*, 229.
(30) Sommer, H. Z.; Lipp, H. I.; Jackson, L. L. *J. Org. Chem.* **1971**, *36*, 824−828.
(31) Wintgens, V.; Amiel, C. *J. Photochem. Photobiol. A* **2004**, *168*, 217−226.
(32) Eftink, M. R.; Andy, M. L.; Bystrom, K.; Perlmutter, H. D.; Kristol, D. S. *J. Am. Chem. Soc.* **1989**, *111*, 6765−6772.
(33) Galant, C.; Wintgens, V.; Amiel, C. *Macromolecules* **2005**, *38*, 5243−5253.
(34) Galant, C.; Amiel, C.; Wintgens, V.; Sébille, B.; Auvray, L. *Langmuir* **2002**, *18*, 9687−9695.
(35) Mukerjee, P.; Mysels, K. *Critical Micelle Concentrations of Aqueous Surfactant Systems*; National Bureau of Standards: Washington, DC, 1971; Vol. 36.
(36) Borue, V. Y.; Erukhimovich. *Macromolecules* **1988**, *21*, 3240−3249.
(37) Ermi, B. D.; Amis, E. J. *Macromolecules* **1997**, *30*, 6937−6942.
(38) Moussaid, A.; Schosseler, F.; Munch, J. P.; Candau, S. J. *J. Phys. II* **1993**, *3*, 573−594.
(39) Shibayama, M.; Tanaka, T. *J. Chem. Phys.* **1995**, *102*, 9392−9400.
(40) Cotton, J.-P.; Lindner, P., Zemb, T., Eds.; *Introduction to scattering experiments in neutron, X-ray and light scattering*: North-Holland Delta Series: Amsterdam, 1991; p 3.
(41) Zeghal, M.; Auvray, L. *Europhys. Lett.* **1999**, *45*, 482.
(42) Daoud, M.; Joanny, J. F. *J. Phys.* **1981**, *42*, 1359−1371.
(43) Muller, F.; Delsanti, M.; Auvray, L.; Yang, J.; Chen, Y. J.; Mays, J. W.; Demé, B.; Tirrell, M.; Guenoun, P. *Eur. Phys. J. E* **2000**, *3*, 45−53.
(44) Nisato, G.; Ivkov, R.; Amis, E. J. *Macromolecules* **1999**, *32*, 5895−5900.
(45) Ramzi, A.; Scherrenberg, R.; Joosten, J.; Lemstra, P.; Mortensen, K. *Macromolecules* **2002**, *35*, 827−833.
(46) Ohshima, A.; Konishi, T.; Yamanaka, J.; Ise, N. *Phys. Rev. E* **2001**, *64*, 051808.
(47) Yun, S. I.; Briber, R. M.; Kee, R. A.; Gauthier, M. *Polymer* **2006**, *47*, 2750−2759.
(48) Borisov, O. V.; Daoud, M. *Macromolecules* **2001**, *34*, 8286−8293.
(49) Jusufi, A.; Likos, C. N.; Löwen, H. *Phys. Rev. Lett.* **2002**, *88*, 018301.
(50) Likos, C. N.; Ballauff, M. *Equilibrium Structure of Dendrimers − Results and Open Questions*, 245 ed.; Springer: New York, 2005.
(51) Galant, C.; Amiel, C. *J. Phys. Chem. B* **2004**, *108*, 19218−19227.
(52) Debye, P. *J. Phys. Colloid Chem.* **1947**, *51*, 18−32.
(53) Goddard, E. D.; Ananthapadmanabhan, K. P. *Interactions of surfactants with polymers and proteins*; CRC Press: Boca Raton, FL, 1993; Chapters 4 and 5.

BM060523K